Journal of Advanced Research in Fluid Mechanics and Thermal Sciences

Journal homepage:
https://semarakilmu.com.my/journals/index.php/fluid_mechanics_thermal_sciences/index
ISSN: 2289-7879

Real-time Thermal Energy Harvesting from Solar Radiation in Malaysia at Low-Temperature Difference

Muhammad Nazri Rejab[1], Omar Mohd Faizan Marwah[1,*], Muhammad Akmal Johar[2], Mohamed Najib Ribuan[3]

[1] Faculty of Mechanical and Manufacturing Engineering, Universiti Tun Hussein Onn, Parit Raja, 86400 Batu Pahat, Johor, Malaysia
[2] Technical Delivery Excellence, Level 21, PETRONAS Tower 3, Persiaran KLCC, Kuala Lumpur City Centre, Kuala Lumpur 50088, Malaysia
[3] Faculty of Electric and Electronic Engineering, Universiti Tun Hussein Onn Malaysia, Parit Raja, 86400 Batu Pahat, Johor, Malaysia

ARTICLE INFO

Article history:
Received 8 April 2023
Received in revised form 16 June 2023
Accepted 21 June 2023
Available online 8 July 2023

Keywords:
Real-time; thermoelectric generator; low temperature

ABSTRACT

Malaysia is located in a tropical climate with an abundance of solar radiation. Due to the low albedo of roofing material, around 20 % to 90 % of heat is absorbed from solar radiation. Thus, it is possible to harvest thermal energy from solar radiation using TEG, which promotes the diversity of renewable energy sources in Malaysia. Previous research evaluates the potential of thermal energy harvesting of the TEG open circuit voltage and unipolar condition. Thereby, this research focuses on designing and developing a thermal energy harvesting system (TEHS) for harvesting thermal energy at low-temperature differences from solar radiation. The TEHS can harvest thermal energy in bipolar conditions, different voltage levels, TEG input voltage fluctuations, and rapid weather-changing conditions during real-time field tests. Parallel with series balance TEG array configuration obtained impedance matching at 125 Ω. The field test method was conducted for 105 days. The maximum mean efficiency obtained is 94.33 %, with an output power range between 0.46 mW and 66.10 mW. The promising finding indicates that the developed TEHS is robust and capable of operating at optimum power transfer at uncontrollable solar radiation and weather conditions. In addition, the potential of the power generated evaluation is to be used as a power supply to several sensor nodes.

1. Introduction

Global warming, environmental pollution, depletion of fuel resources and the increase in electricity generation attract researchers to discover a solution to harvest energy, especially from natural sources such as solar, vibration, flow, and thermal energy [1,2]. Solar energy is a common energy source for harvesting using a solar cell. Combining multiple solar cells into solar panel modules can increase the power output. An advanced design method, which is cross-layer optimization, can be used to improve the individual solar cell's optimum power output [3]. Further, the optimum power output by solar cells depends on the cell size, efficiency, and light intensity. The solar cell's efficiency, cost and flexibility depend on the fabrication material. The power conversion efficiency of solar cells

---

[*] *Corresponding author.*
E-mail address: faizan@uthm.edu.my

https://doi.org/10.37934/arfmts.107.2.117132

is classified according to the type of material, which is polycrystalline (14-20.4%), monocrystalline (15-24%), and thin-film (8-13.2%) [4,5]. Another energy source that can be harvested from solar is thermal energy. Typically, a thermoelectric generator (TEG) is used to harvest thermal energy from solar radiation [6]. Their use is becoming of more interest as they offer the advantages of harvesting thermal waste energy, such as no moving part, long lifetime, and highly reliable [7,8].

On the other hand, Malaysia is located in a tropical climate with a solar radiation range of 4.21 kWh/m^2 to 5.56 kWh/m^2 per year [9,10]. In 1998, the peak daily temperature recorded was 40.1 °C in Chuping. In 2020, the peak temperature was 38.6 °C in Alor Setar, declared by Malaysian Meteorological Department [11]. A temperature difference (ΔT) below 20 °C is available and considered low. Therefore, the potential of the low-temperature difference should be evaluated, not wasted. Research by Gunawan *et al.,* [12] recorded the daily temperature is 53 °C in Bogor, Indonesia. The temperature value indicates the potential of thermal energy harvesting in other Asian countries. In Malaysia, 76 % of solar thermal energy is obtained from the roof [13]. Whereby the roofing surface absorbs 20 % to 90 % solar radiation at 1 kWh/m^2 during bright weather conditions [14].

In 2014, Malaysia launched the National Internet of Things Strategic Roadmap in the domestic market in addition to the 2030 Sustainability Goal introduced to reduce 25 % of gross electricity consumption from the building sector by employing sensor node (SN) in the energy control system [15-18]. The SN energy consumption depends on the stage of operation [19,20]. Alternatively, thermal energy can power the SN or charge the energy storage devices, such as batteries or capacitors [21]. It has reduced the SN's installation, maintenance, and wiring costs [22]. The research in SN improves its performance while reducing energy consumption. Power sources in various sectors use electrical energy from thermal energy harvesting [23]. TEG obtains higher performance at the high-temperature difference, which is suitable for industrial implementations. Thus, it has the capability of use as a power supply to the SN or IoT applications, as shown in Figure 1.

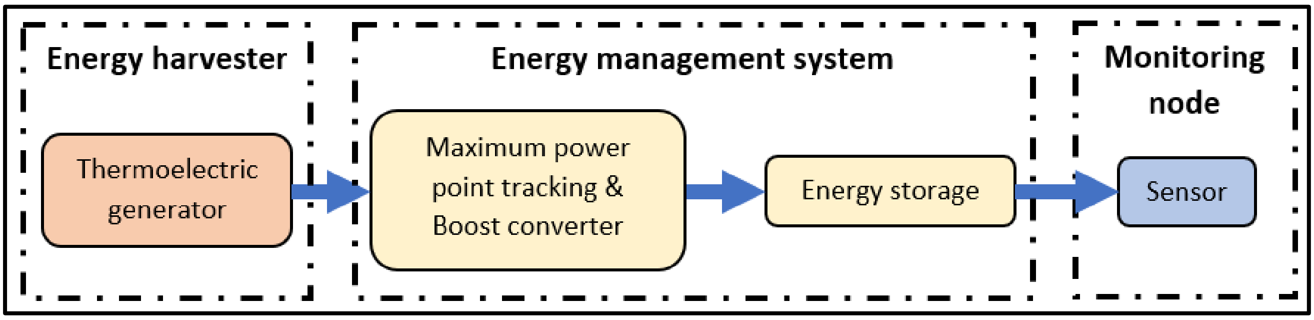

Fig. 1. The block diagram of TEG to power the sensor node

Further, researchers in Malaysia conducted research to harvest thermal energy from solar radiation, such as asphalt, PV-TEG, shingle, and solar pond, as listed in Table 1. However, the research only measures open circuit voltage from the TEG and thermal energy harvesting system (TEHS) capable of unipolar conditions. Thereby, designing and developing a bipolar TEHS circuit is compulsory due to the unique character of the TEG module. In addition, the TEHS must be capable of adapting to temperature fluctuation, bipolar conditions, and rapid temperature changes in real-time implementation. The output power from the TEG is proportional to the temperature difference between the hot and cold sides. At low-temperature differences, the output power is too small to utilize. Therefore, a DC boost converter is needed to increase the output power from the TEG [24].

Table 1
Research on thermal energy harvesting from solar radiation

No.	Application	Type	ΔT, °C	TEHS	Year	Ref.
1	Asphalt	Real-time	23	BQ25505	2021	Khamil *et al.,* [25]
2	Asphalt	Real-time	7.95	ECT 310	2020	Khamil *et al.,* [26]
3	PV-TEG	Experimental	8	No	2019	Shatar *et al.,* [9]
4	PV-TEG	Numerical	56.1	No	2019	Ruzaimi *et al.,* [27]
5	Asphalt	Experimental	2.49	No	2019	Sharuddin *et al.,* [28]
6	Asphalt	Experimental	29.77	No	2019	Khamil *et al.,* [29]
7	Shingle	Experimental	3	No	2017	Johar *et al.,* [30]
8	Solar pond	Simulation	40 to 100	No	2017	Baharin *et al.,* [31]
9	PV-TEG	Experimental	10 to 40	No	2012	Daud *et al.,* [32]

The remaining sections of this article organize as follows. First, section 2 describes the methodology to harvest thermal energy in real-time implementation. Next, the result of thermal energy harvesting using TEHS describes in Section 3. The final Section 4 brings the conclusions and recommendations for future work.

2. Methodology

2.1 Real-time Experiment Setup

The real-time experimental setup of the TEG module is present in Figure 2. TEC1-12706 is used as the TEG module. The specifications of the TEG module are listed in Table 2. The TEG array configuration is parallel with the series balance connection of the 192 TEG module. The 96 TEG modules are in series connection for each connection, as depicted in Figure 3. The TEG hot side is attached to the metal deck, and the cold side is to the heatsink. To improve the thermal conductivity, a thin layer of thermal cooler (Cooler Master HTK-002) is used on the TEG surface and the aluminium heatsink. The thermal paste properties are listed in Table 3. The heatsink is used to dissipate the heat on the cold side by nature wind blowing.

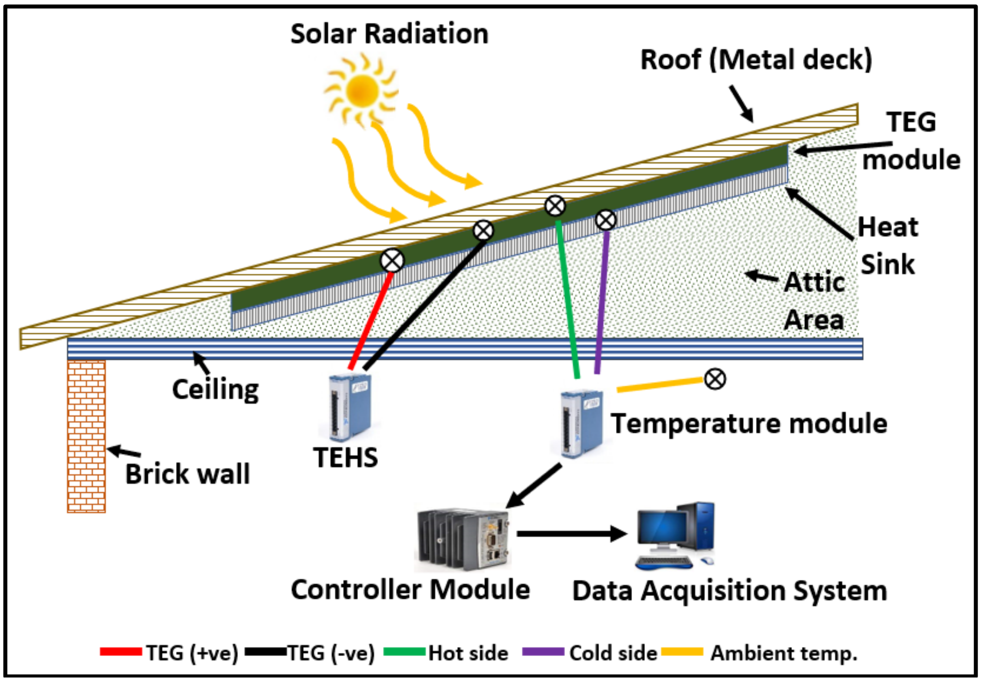

Fig. 2. The real-time experiment setup

Table 2
The specification of the TEC1-12706 [33]

Description	Value	Value
Hot side temperature (°C)	25 °C	50 °C
Q_{MAX} (watts)	50	57
Delta T_{MAX} (°C)	66	75
I_{MAX} (Amps)	6.4	6.4
V_{MAX} (Volts)	14.4	16.4
Module resistance (Ohms)	1.98	2.30

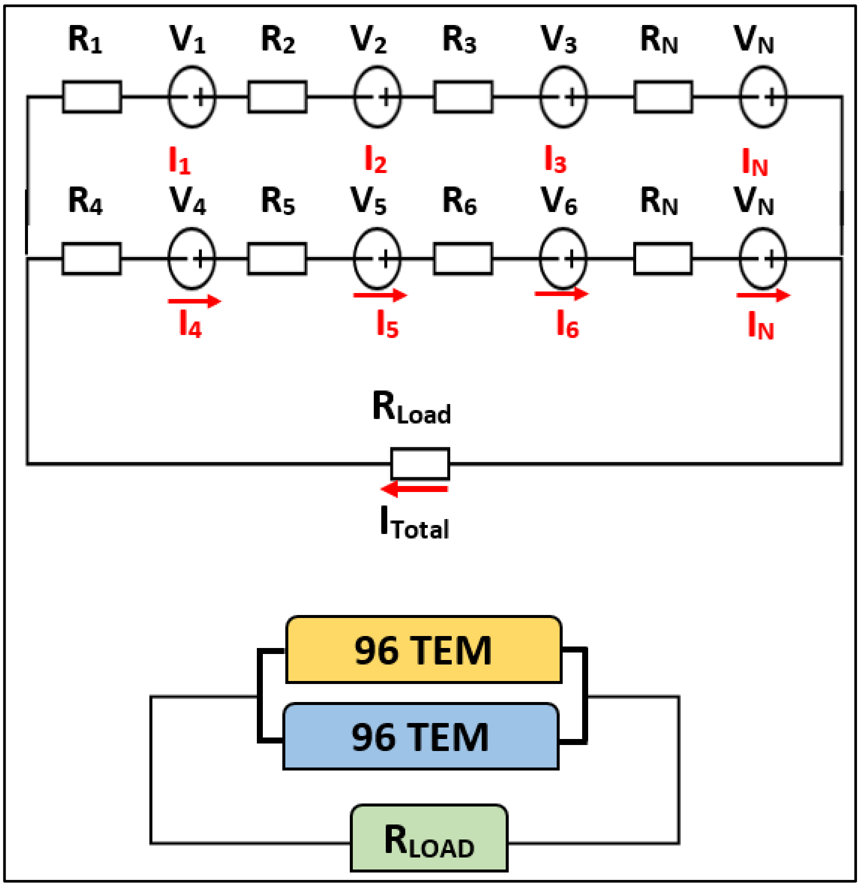

Fig. 3. The parallel with series balance TEG array configuration

Table 3
Properties of Cooler Master HTK-002

Description	Properties
Type	Cooler Master (HTK-002)
Colour	White
Viscosity/Flowability	Non-flowing
Dielectric constant	4.4 at 100 kHz
Volume resistivity	5.0×10^{15}
Dissipation factor	0.02 at 100 kHz
Dielectric strength	550 volts/mil;21.7kV/mm
Thermal conductivity	0.8 watts/meter-°C

NI-9211 is the temperature module to record the hot and cold side TEG and ambient temperatures. First, it measured the temperature data using a type-K thermocouple as the temperature sensor. Then, the temperature module is attached to the controller module (NI cRIO-

9014 RT) and synchronous with the data acquisition system (DAQ) to record all the real-time temperature data using LabVIEW software. The LabVIEW layout is portrayed in Figure 4. The variables and device properties are listed in Table 4.

Table 4
The variable and device properties used in this research

No.	Variable	Sensor / Module	Description
1	Temperature	Thermocouple	Type-K -200 to 1200 °C Accuracy (+/- 2.2 °C or +/- 0.75 %) JUMO Instrument Co. Ltd
2	Temperature	NI-9211	Anti-aliasing Open-thermocouple tracking Operating Temp. range (-40 °C to 70 °C) National Instruments
3	DAQ	NI cRIO-9014 RT Controller module	Memory (2GB) Internal real-time clock accuracy (200 ppm, 35 ppm at 25 °C) Ethernet network (RJ-45) National Instruments

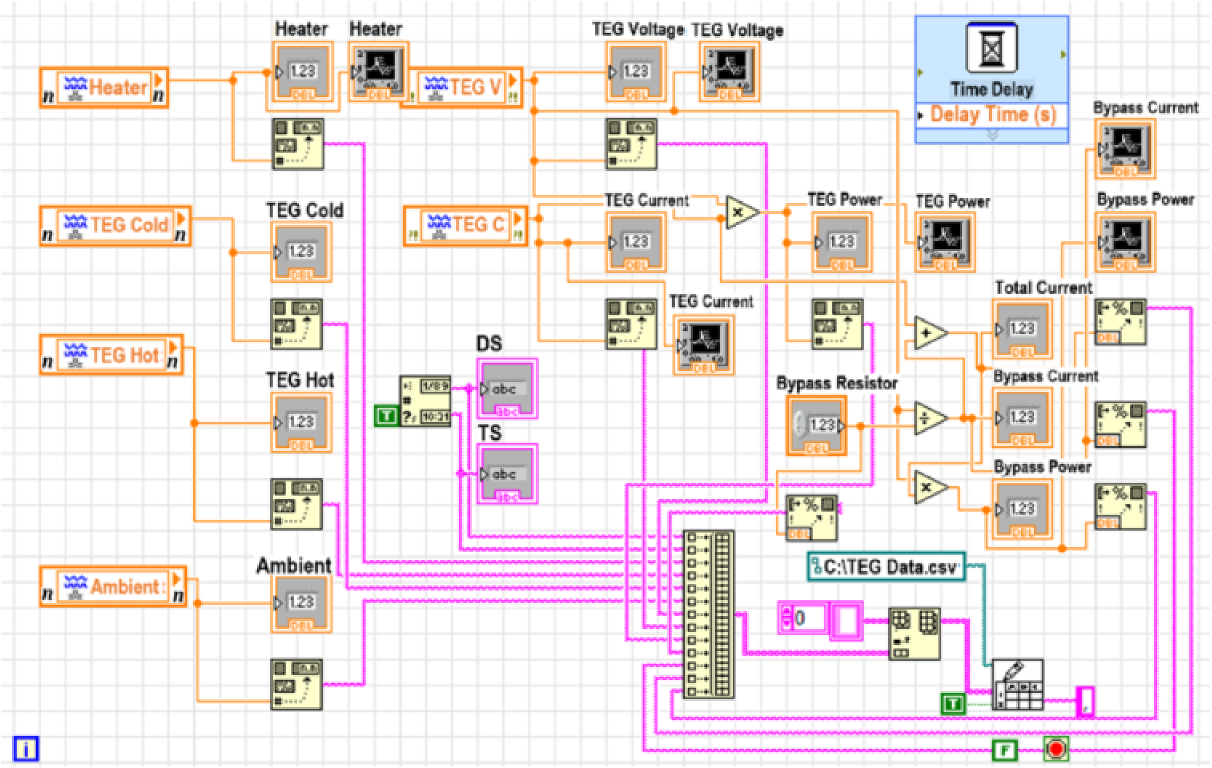

Fig. 4. The LabVIEW layout to recoded real-time temperature data

2.2 Real-time Temperature Data Analysis

Figure 5 shows the real-time temperature data distribution for three days. The temperature criteria are rapidly changing, bipolar conditions, and temperature fluctuation. The bipolar condition occurs from the TEG module's unique characteristic and should be considered in the data analysis. The absolute data analysis (ADA) method is used to analyze the overall data. Further, the ADA method can analyze mixed-mode data compared to the conventional method. Using the conventional method, the exact point-to-point of transition and intersection points needs to determine along the data analysis.

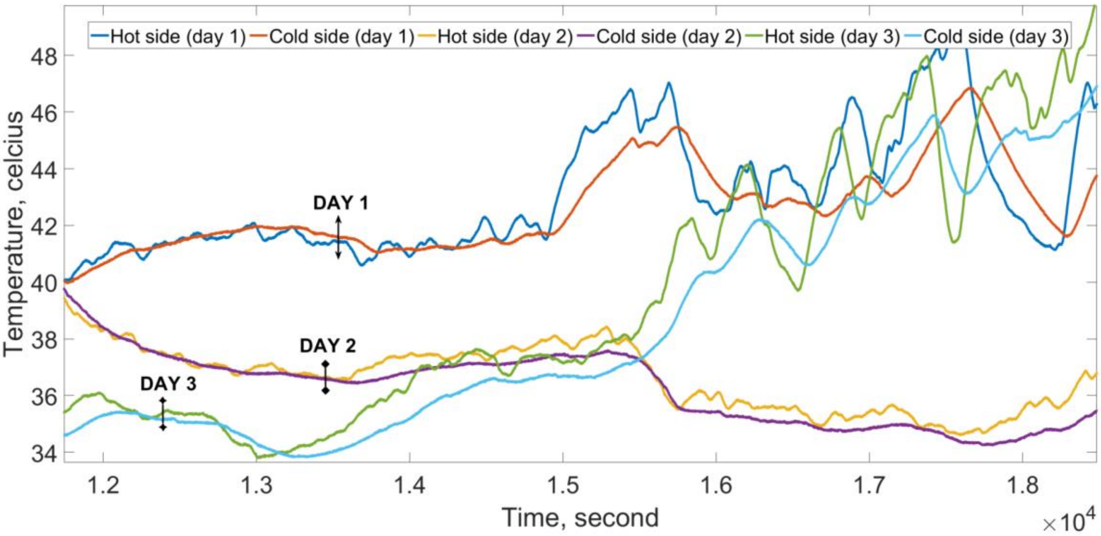

Fig. 5. Real-time temperature data measured from the experiment

ADA method is designed in the MATLAB Simulink software to process the real-time data. First, the real-time temperature data is converted to a time series data arrangement, as shown in Figure 6, to enable simultaneous data recording with synchronous data management using the 'from workspace' and 'to workspace' block in the developed simulation system. Thus, the ADA method simultaneously processes all the real-time data at different criteria.

The ADA method is combined with the TEG equivalent circuit to enhance the real-time data analysis and eradicate the intersection point error through the temperature fluctuation data, as shown in Figure 7. The data processing system synchronizes the input and output data using the 'to workspace' block.

```
Time = 0:1:2106;
Time = transpose (time);
TEG1 = [time TEG];
```

Fig. 6. Time-series conversion step of real-time temperature data

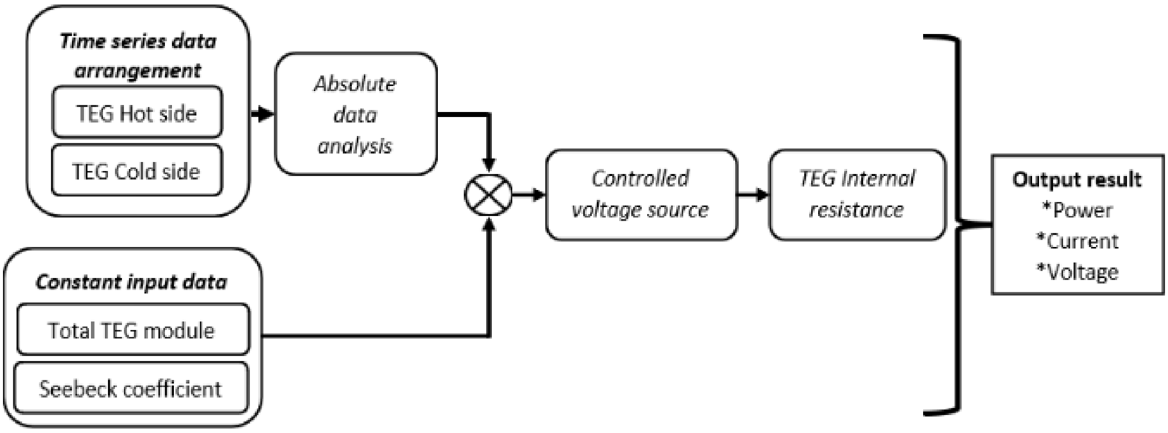

Fig. 7. The combination of time series data and the ADA method

2.3 Thermal Energy Harvesting System

The TEHS design combines several modules, as presented in Figure 8. The TEHS is designed and developed using Proteus software. The selection of each component used on the circuit board goes through comprehensive experimental testing to evaluate each module.

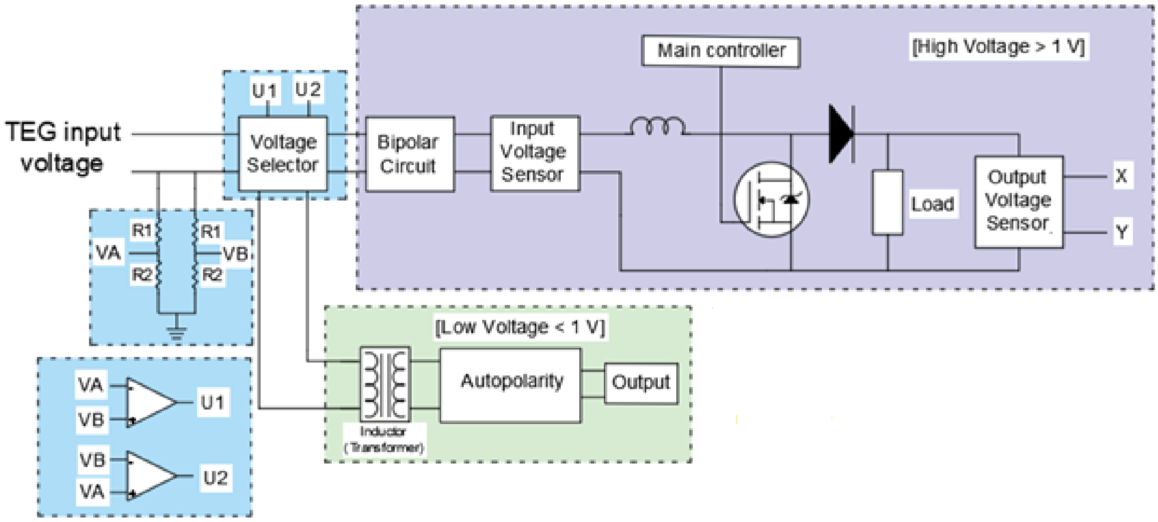

Fig. 8. The schematic diagram of the thermal energy harvesting system

Furthermore, the SD card module stores the input data from the TEG. An interesting feature of this TEHS is the bipolar capability to harvest the energy of rapidly changing TEG input voltage. This bipolar circuit changes the TEG input's reverse polarity to constant polarity before the DC boost converter circuit. Then, the low voltage level TEG input is switched to the low-side integrated circuit that can produce 5-volt output. The efficiency of the TEHS is determined using Eq. (1).

$$\eta_{TEHS} = \frac{P_{out}}{P_{TEG}} x\ 100 \tag{1}$$

where P_{OUT} and P_{TEG} are the output power of the TEHS and TEG input power, respectively. In addition, the optimum power transfer occurs when the TEG internal resistance equals load resistance. The topology of the circuit operation is discussed below:

Stage 1:

The TEG input voltage is a random value dependent on solar radiation and environmental condition. It consists of low, high, and bipolar conditions. Two operational amplifiers, U1 and U2, are used to detect the input value's level and condition, capable of categorizing the input. It received the signal from V_A and V_B connected to the TEG input voltage with a voltage divider circuit. The value of R1 and R2 depends on the TEG input voltage. U1 and U2 transmit the data to the main controller when the input value is confirmed. The main controller triggers the selector relay accordingly based on the programming setup. The initial position of the relay is connected to the low-voltage level circuit. When the voltage reaches a high voltage level, the relay automatically switches to the high voltage level circuit.

Stage 2:
The low voltage level circuit (0 to 1 volt) consists of an inductor transformer integrated with a specified capacitor value. LTC 3109 plays a role in receiving and processing the input voltage value and amplifying output to 5 volts.

Stage 3:
The high voltage level goes to the bipolar circuit before the DC boost converter. Two voltage sensors at the input and output sense the voltage value and transmit it to the main controller. Then the main controller's maximum power point tracking (MPPT) algorithm tracks the maximum power point (MPP).

Stage 4:
Both low- and high-voltage circuit outputs charge the battery.

3. Results and Discussion

3.1 Real-time Temperature Data

The real-time temperature characteristic for one day (24 hours) is portrayed in Figure 9. The temperature data was recorded at every second interval to increase the accuracy for further analysis. The hot and cold side temperatures are considered to evaluate TEG for thermal energy harvesting. The real-time temperature data is divided into morning (12.00 midnight – 6.00 a.m.), day (6.00 a.m. – 6.00 p.m.), and evening (6.00 p.m. – 12.00 midnight). The day temperature indicated higher temperatures than the morning and evening sections. The temperature decreases slowly in the evening section proportional to the solar radiation level. However, heat is still available at the roof material due to the low albedo characteristic of the materials. Details explanation of each section's real-time temperature characteristic as the following. Three days of temperature data are taken as examples to compare for each section.

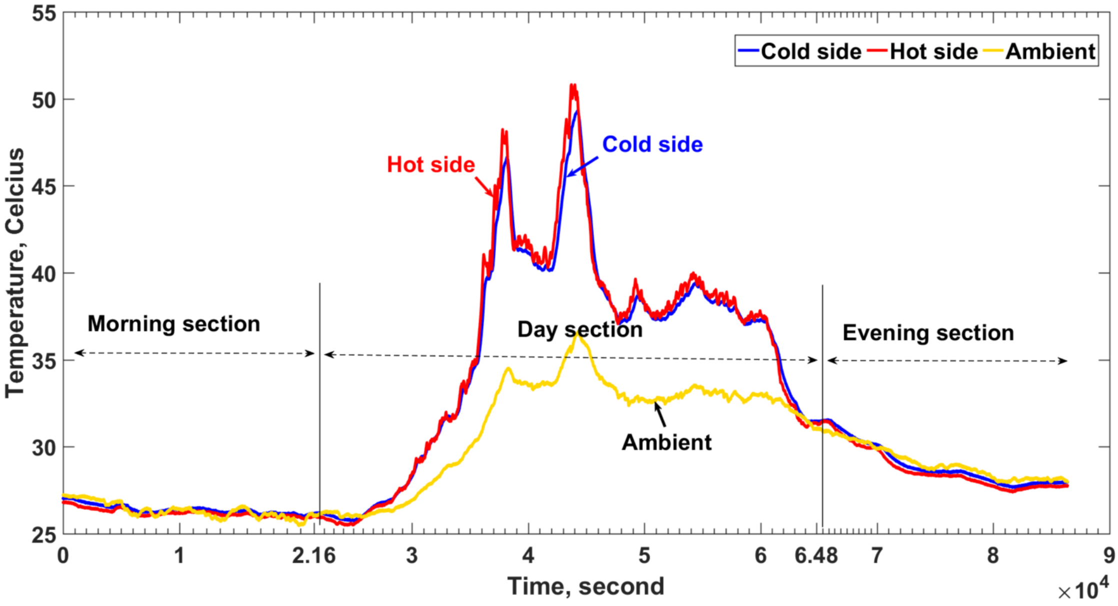

Fig. 9. Real-time temperature characteristic

Figure 10 presents the morning section temperature data. It indicates that the highest temperature is 28.0 °C on day 2. Followed by day 1 at 27.0 °C and day 3 at 26.8 °C. In this section, the temperature data show unique characteristics, where the hot side value is lower than the cold side value of all three days. Thereby, the polarity of TEG is in reverse condition. The temperature decreases proportionally towards 6.00 a.m., and it tends to stabilize from 25.5 °C to 26.5 °C.

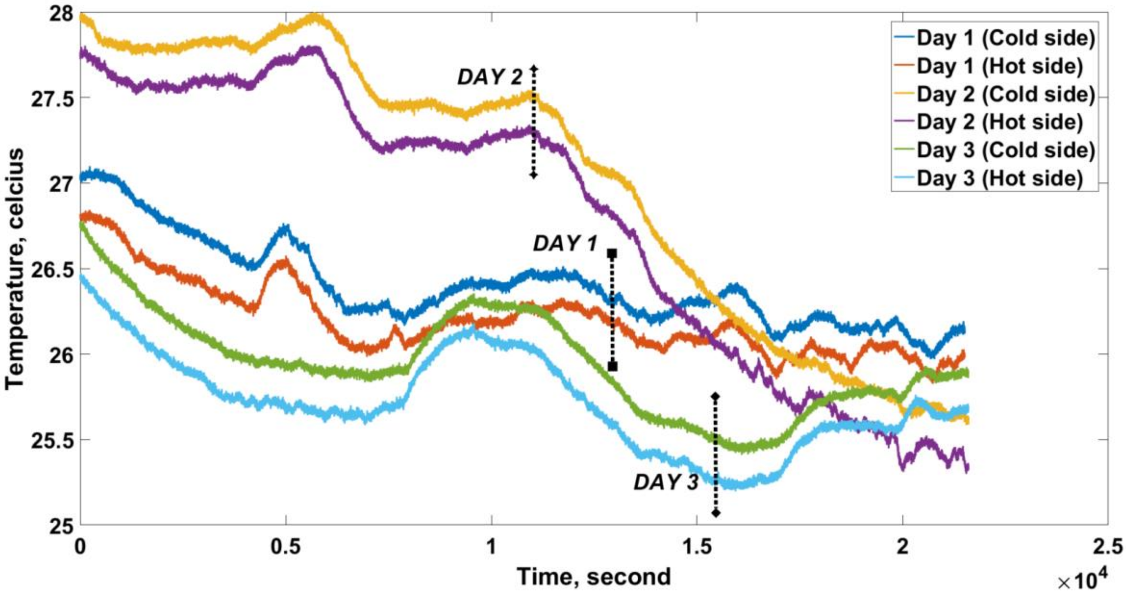

Fig. 10. Temperature of the morning section

Furthermore, the evening section temperature value is higher than the morning section due to the capability of the roof materials to store thermal energy, as shown in Figure 11. The highest temperature value is 33 °C on day 3. While day 1 obtained 31.5 °C and day 2 at 29.0 °C. Interestingly, the temperature difference is still available at midnight. Even though the temperature difference is slight, further research can be conducted to evaluate the potential of harvesting thermal energy.

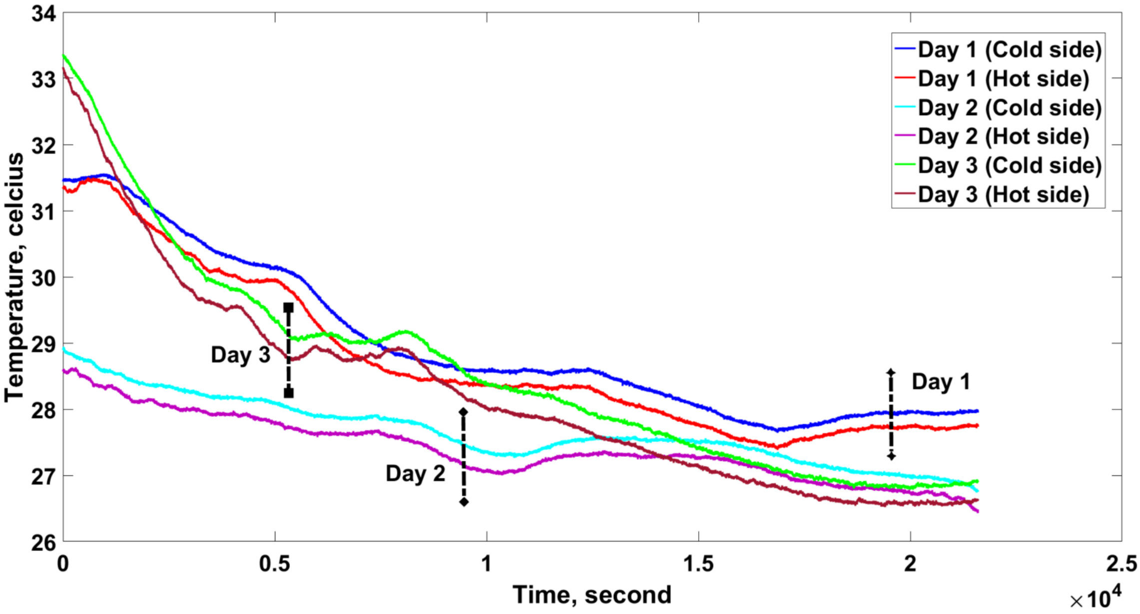

Fig. 11. Temperature of the evening section

The day section indicated complicated temperature values depending on the amount of solar radiation and the weather condition as portrayed in Figure 12. Significant effects of both factors can be seen from the temperature distribution. Most temperature fluctuation is at mixed mode conditions (positive and negative temperature difference). It will affect the input voltage from the TEG to the TEHS. Therefore, to harvest the thermal energy, the TEHS must be capable of operating in bipolar conditions. The highest temperature value was obtained on day 3 at 55 °C, followed by day 1 at 50 °C and day 2 at 47 °C. As mentioned before, this condition is not fixed because it depends on both factors. However, the temperature difference is higher than morning and evening sections. In addition, the TEG's input voltage range is separated into two levels (< 1 volt or ≥ 1 volt). Thus, the TEHS is designed to operate at both voltage levels.

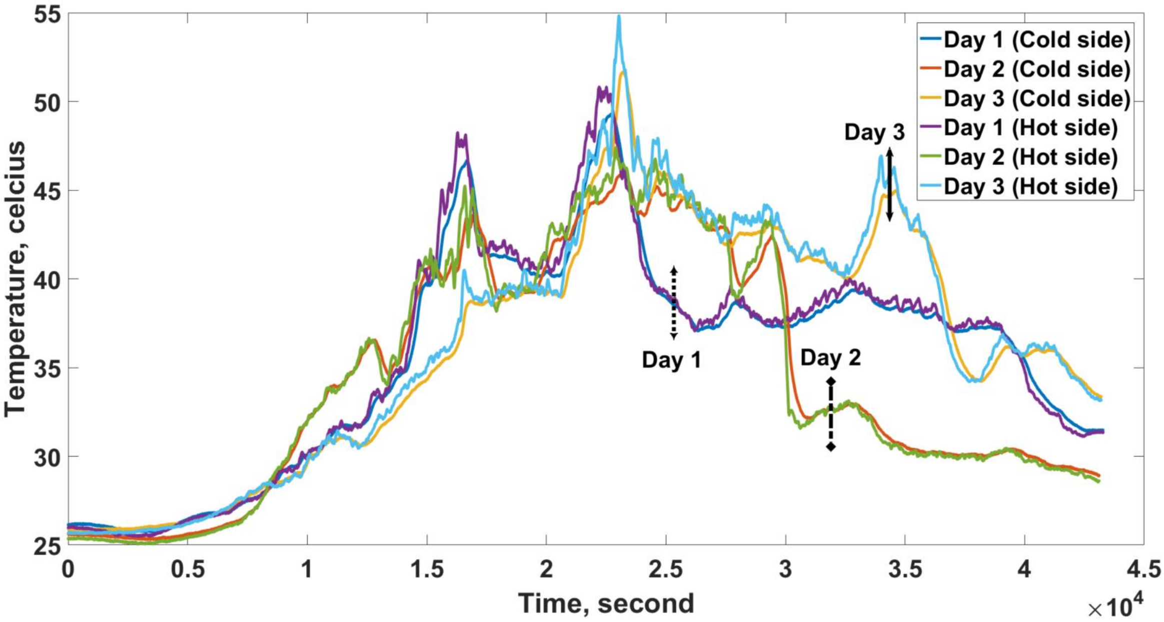

Fig. 12. Temperature of the day section

From the 20 days of temperature data, the temperature difference of all sections is listed in Table 5. The temperature in the morning section ranges from 0.332 °C to 0.487 °C. The evening section is from 0.340 °C to 0.784 °C and day section range from 2.001 °C to 5.580 °C.

Table 5
The maximum temperature difference for each section

Day	Morning (°C)	Evening (°C)	Day (°C)	Day	Morning (°C)	Evening (°C)	Day (°C)
1	0.362	0.459	3.154	11	0.417	0.376	5.580
2	0.361	0.352	4.591	12	0.379	0.403	5.472
3	0.332	0.502	4.194	13	0.392	0.436	2.001
4	0.417	0.471	4.264	14	0.368	0.490	2.900
5	0.412	0.644	4.346	15	0.448	0.481	3.783
6	0.422	0.778	2.767	16	0.444	0.543	3.824
7	0.361	0.589	3.190	17	0.447	0.483	3.496
8	0.353	0.542	3.886	18	0.421	0.375	3.510
9	0.457	0.784	5.271	19	0.414	0.506	4.808
10	0.487	0.507	2.280	20	0.462	0.340	3.922

3.2 Impedance Matching

Further, the output power of different load values of the parallel with series balance TEG array configuration is present in Figure 13. The highest output power was obtained at 125 Ω (0.94 Watt), followed by 90 Ω (0.91 Watt), 200 Ω (0.89 Watt), 250 Ω (0.84 Watt), 503 Ω (0.60 Watt), and 600 Ω (0.54 Watt). The circuit testing using different load resistance values determines the external load to achieve impedance matching. Thereby, the output power of 125 Ω obtained optimum power transfer. At this load resistance value, the TEG internal resistance equals the external load resistance, thus achieving the impedance matching conditions. However, it will limit the implementation of thermal energy harvesting concerning external load resistance. Therefore, the MPPT algorithm should implement in the TEHS circuit to increase the external load value to address this issue. Thereby the capability of the TEHS to harvest thermal energy with variable values of external load achieve.

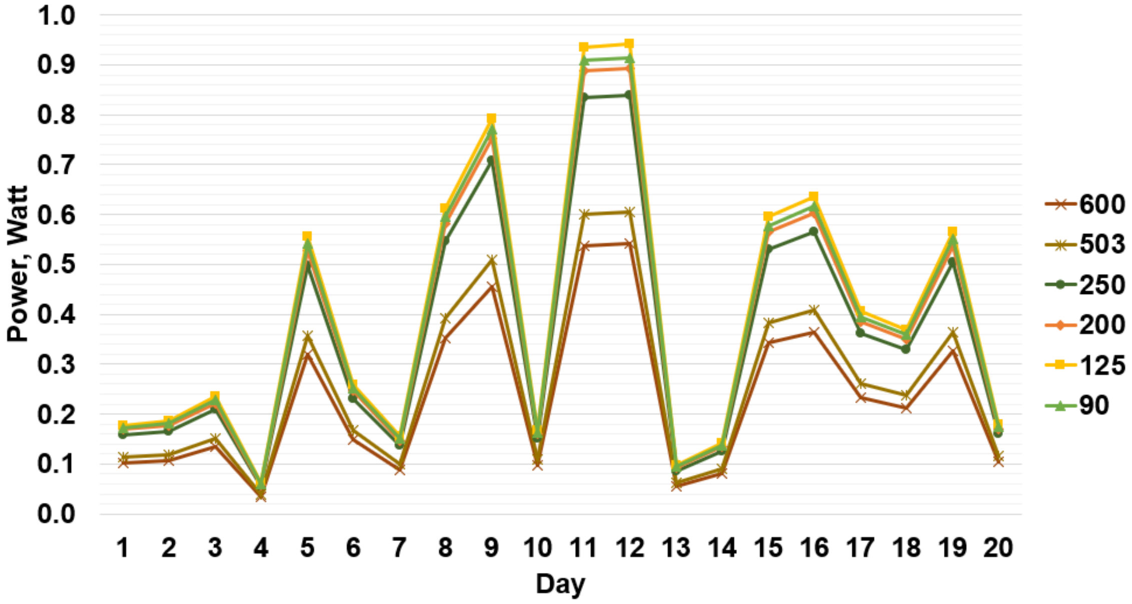

Fig. 13. The impedance matching of output power

3.3 Thermal Energy Harvesting System

The TEHS is tested in the field test (real-time experiment) to evaluate the mean efficiency of the TEHS. From the field test, the maximum mean efficiency obtained is 94.33 % of 105 days, as shown in Figure 14. The mean efficiency indicated that the TEHS could operate in various temperature fluctuations, bipolar conditions, and rapid temperature fluctuation. However, solar radiation and weather conditions affect the field test on certain days. Whereby this condition is uncontrollable. The lowest mean efficiency is on day 9 at 89.62 %, and the rest is above 90 %.

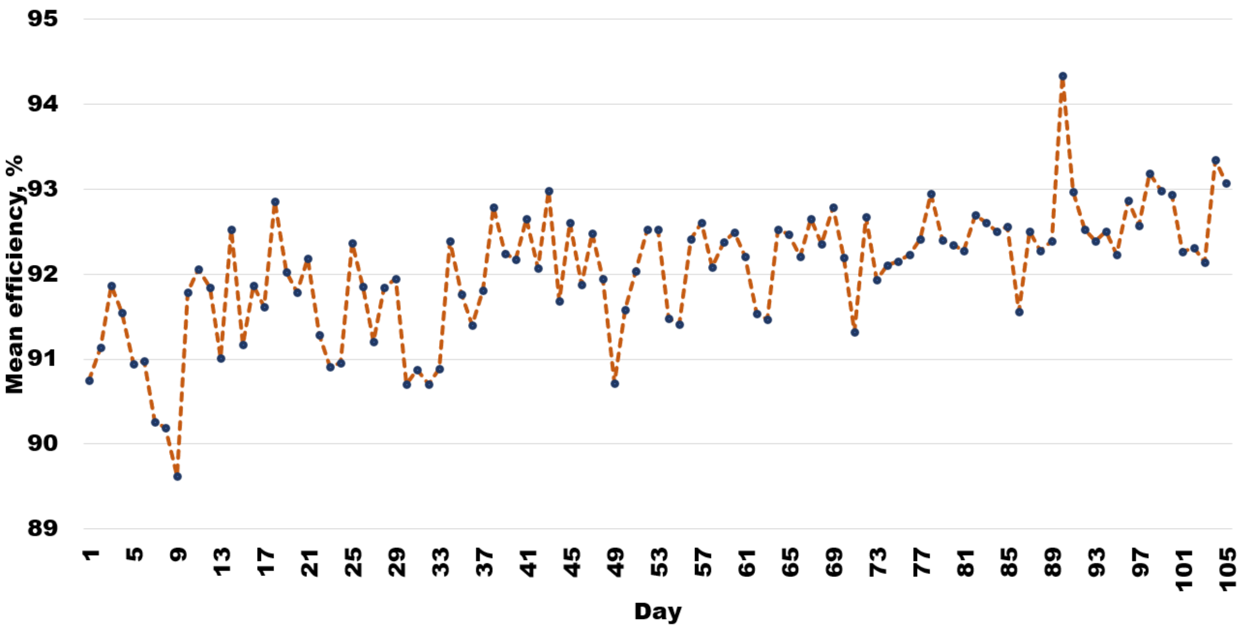

Fig. 14. The mean efficiency of TEHS

Furthermore, the input and output power are present in Figure 15. The maximum output power range is from 0.46 mW to 66.10 mW. Based on the SN power requirement from microwatts (μW) to milliwatts (mW) power consumption in operating modes (sleep, idle, transmit and receive), the minimum output power can be used as the power supply for the SN [34]. Table 6 lists the power requirement by the typical SN. The SN's potential, amount and durability have become an interesting topic for further research, especially in Malaysia's environment. On the other hand, the comparison of the TEHS with other researches are in Table 7.

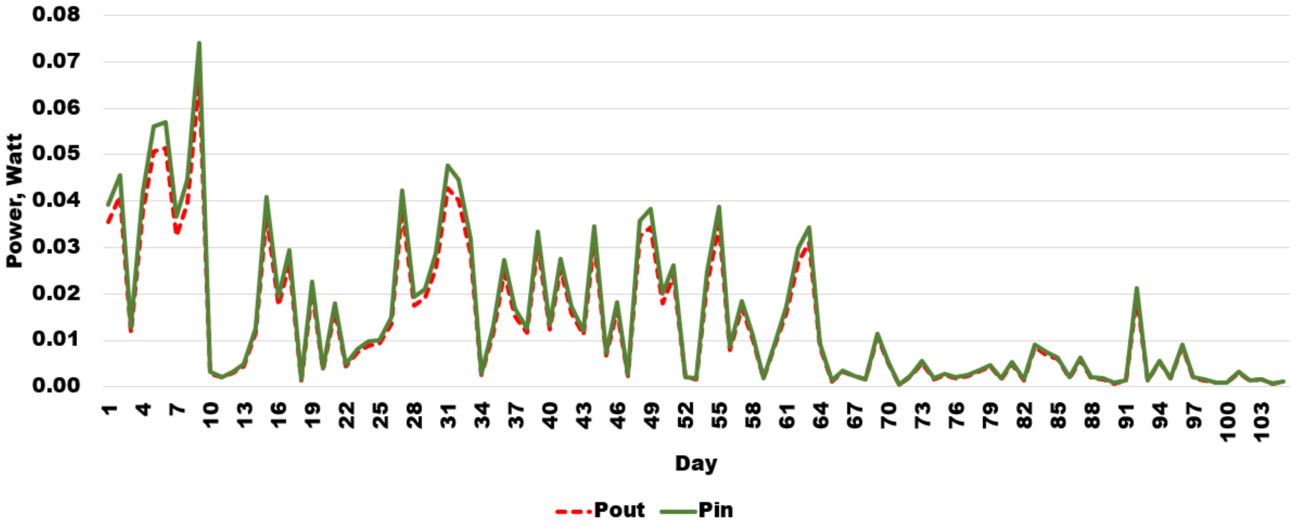

Fig. 15. The real-time input and output power

Table 6
The sensor node power requirement

Component	Average power	Ref.
Temperature measurement	720 µW	Charris *et al.,* [35]
Humidity sensor	480 µW	Charris *et al.,* [35]
Microcontroller (processing)	528 µW	Charris *et al.,* [35]
Daylight sensor	21 µW	Hidalgo-Leon *et al.,* [34]
Temperature sensor	0.6 µW	Hidalgo-Leon *et al.,* [34]
Ambient light, temperature, humidity	1.25 mW	Hidalgo-Leon *et al.,* [34]
Light, presence, and temperature	0.34 µW	Hidalgo-Leon *et al.,* [34]

Table 7
Comparison of TEHS at the low-temperature difference

Ref.	Kimura and Koizumi [36]	Taeda and Koizumi [37]	Taeda *et al.,* [38]	Kimura *et al.,* [39]	This research
ΔT, °C	NA	9.5	4 & 12	5	6
Vin, Volt	+ 1 & - 1	0.7	-1.73 & -0.238	+1.5 & -1.5	1>Vin≥1
Vout, Volt	2.4	2.4	1.2	2.4	4
Polarity	Bipolar	Bipolar	Bipolar	Bipolar	Bipolar
Application	Experiment	Experiment	Experiment	Experiment	Real-time
DC converter	Boost	Boost	Buck- Boost	Boost	Boost
MPPT	Yes	Yes	Yes	Yes	Yes

NA (not applicable)

4. Conclusions

The potential of temperature difference from solar radiation evaluates for 20 days. The day section indicated a significant temperature difference compared to the evening and morning sections. The maximum temperature difference in the morning section is 0.487 °C, the evening section is 0.784 °C, and the day section is 5.580 °C. The impedance matching condition evaluates using MATLAB Simulink software at different load resistance ranges (600 Ω, 503 Ω, 250 Ω, 200 Ω, 125 Ω, and 90 Ω). In addition, the ADA method integrated with the time series data arrangement and synchronous data management can analyze temperature fluctuation, mixed data (positive and negative value) and bipolar conditions of temperature fluctuation. Based on the result, the impedance matching obtained at 125 Ω of parallel with series balance TEG array configuration. The TEHS obtained mean efficiency of 94.33 % at the field test for 105 days with a maximum output power range from 0.46 mW to 66.1 mW. The potential of thermal energy harvesting from solar radiation for SN power consumption is achieved, and further research on integrated TEHS with SN is interesting.

Acknowledgement

This research was funded by the Ministry of Higher Education (MOHE) through the Fundamental Research Grant Scheme (FRGS/1/2018/TK10/UTHM/02/2) or Vot No. K108.

References

[1] Samsudin, Muhammad Syazwan Nizam, Md Mizanur Rahman, and Muhamad Azhari Wahid. "Sustainable power generation pathways in Malaysia: Development of long-range scenarios." *Journal of Advanced Research in Applied Mechanics* 24, no. 1 (2016): 22-38.

[2] Jiao, Pengcheng, Wassim Borchani, Hassene Hasni, and Nizar Lajnef. "Enhancement of quasi-static strain energy harvesters using non-uniform cross-section post-buckled beams." *Smart Materials and Structures* 26, no. 8 (2017): 085045. https://doi.org/10.1088/1361-665X/aa746e

[3] Prauzek, Michal, Jaromir Konecny, Monika Borova, Karolina Janosova, Jakub Hlavica, and Petr Musilek. "Energy harvesting sources, storage devices and system topologies for environmental wireless sensor networks: A review." *Sensors* 18, no. 8 (2018): 2446. https://doi.org/10.3390/s18082446

[4] Panatik, Kamarul Zaman, Kamilia Kamardin, Sya Azmeela Shariff, Siti Sophiayati Yuhaniz, Noor Azurati Ahmad, Othman Mohd Yusop, and SaifulAdli Ismail. "Energy harvesting in wireless sensor networks: A survey." In *2016 IEEE 3rd International Symposium on Telecommunication Technologies (ISTT)*, pp. 53-58. IEEE, 2016. https://doi.org/10.1109/ISTT.2016.7918084

[5] Akhtar, Fayaz, and Mubashir Husain Rehmani. "Energy replenishment using renewable and traditional energy resources for sustainable wireless sensor networks: A review." *Renewable and Sustainable Energy Reviews* 45 (2015): 769-784. https://doi.org/10.1016/j.rser.2015.02.021

[6] Rejab, Muhammad Nazri, Omar Mohd Faizan Marwah, Muhammad Akmal Johar, and Mohamed Najib Ribuan. "Dual-Level Voltage Bipolar Thermal Energy Harvesting System from Solar Radiation in Malaysia." *Sustainability* 14, no. 19 (2022): 12521. https://doi.org/10.3390/su141912521

[7] Mahmoudinezhad, S., P. A. Cotfas, Daniel Tudor Cotfas, L. A. Rosendahl, and Alireza Rezania. "Response of thermoelectric generators to Bi2Te3 and Zn4Sb3 energy harvester materials under variant solar radiation." *Renewable Energy* 146 (2020): 2488-2498. https://doi.org/10.1016/j.renene.2019.08.080

[8] Zoui, Mohamed Amine, Saïd Bentouba, John G. Stocholm, and Mahmoud Bourouis. "A review on thermoelectric generators: Progress and applications." *Energies* 13, no. 14 (2020): 3606. https://doi.org/10.3390/en13143606

[9] Shatar, Nursyahirah Mohd, Mohd Azizi Abdul Rahman, Mohd Nabil Muhtazaruddin, Sheikh Ahmad Zaki Shaikh Salim, Baljit Singh, Firdaus Muhammad-Sukki, Nurul Aini Bani, Ahmad Shakir Mohd Saudi, and Jorge Alfredo Ardila-Rey. "Performance evaluation of unconcentrated photovoltaic-thermoelectric generator hybrid system under tropical climate." *Sustainability* 11, no. 22 (2019): 6192. https://doi.org/10.3390/su11226192

[10] Lee, Yee Yong, Mohd Fadhil Md Din, Kenzo Iwao, Yeong Huei Lee, and Nickholas Anting. "Impact of thermal behaviour of different environmental conditions on ambient environment and thermal discomfort in Malaysia." *Indoor and Built Environment* 30, no. 4 (2021): 520-534. https://doi.org/10.1177/1420326X19897956

[11] Dahim, Mohammed, Syed Ahmad Farhan, Nasir Shafiq, Hashem Al-Mattarneh, and Rabah Ismail. "Thermal-Energy Performance of Bulk Insulation Coupled with High-Albedo Roof Tiles in Urban Pitched Residential Roof Assemblies in the Hot, Humid Climate." *Sustainability* 14, no. 5 (2022): 2867. https://doi.org/10.3390/su14052867

[12] Gunawan, Yohanes, Vetri Nurliyanti, Novan Akhiriyanto, Slamet Kasbi, Khalif Ahadi, Muhammad Nabil Makarim Rizkillah, and Muhammad Rizal Fadilah Permana. "A Comparative Study of Photovoltaic Water Pumping System-Driving Conventional AC Single-phase and Three-phase Motor Submersible Pumps." *Joint Journal of Novel Carbon Resource Sciences & Green Asia Strategy* 9, no. 3 (2022): 893-902. https://doi.org/10.5109/4843121

[13] Nasir, M. Ahmad, C. H. Lim, and A. F. Abdullah. "Survey on the Empirical Method to Evaluate the Thermal Performance of Roof Assembly." In *Journal of Physics: Conference Series*, vol. 1358, no. 1, p. 012040. IOP Publishing, 2019. https://doi.org/10.1088/1742-6596/1358/1/012040

[14] Rawat, Mohan, and R. N. Singh. "A study on the comparative review of cool roof thermal performance in various regions." *Energy and Built Environment* 3, no. 3 (2022): 327-347. https://doi.org/10.1016/j.enbenv.2021.03.001

[15] Badarudin, Ummi Wahida, W. I. S. W. Din, Yuli Adam Prasetyo, Zalili Musa, and Shahreen Kasim. "Internet of Things: An implementation and its challenges in Malaysia." *International Journal on Advanced Science, Engineering and Information Technology* 8, no. 6 (2018): 2641-2647. https://doi.org/10.18517/ijaseit.8.6.5043

[16] Al Musleh, Mohamed, Evangelia Vasiliki Topriska, David Jenkins, and Edward Owens. "Thermoelectric generator characterization at extra-low-temperature difference for building applications in extreme hot climates: Experimental and numerical study." *Energy and Buildings* 225 (2020): 110285. https://doi.org/10.1016/j.enbuild.2020.110285

[17] Shah, Abdul Salam, Haidawati Nasir, Muhammad Fayaz, Adidah Lajis, and Asadullah Shah. "A review on energy consumption optimization techniques in IoT based smart building environments." *Information* 10, no. 3 (2019): 108. https://doi.org/10.3390/info10030108

[18] Shapi, Mel Keytingan M., Nor Azuana Ramli, and Lilik J. Awalin. "Energy consumption prediction by using machine learning for smart building: Case study in Malaysia." *Developments in the Built Environment* 5 (2021): 100037. https://doi.org/10.1016/j.dibe.2020.100037

[19] Zaman, Noor, Low Tang Jung, and Muhammad Mehboob Yasin. "Enhancing energy efficiency of wireless sensor network through the design of energy efficient routing protocol." *Journal of Sensors* 2016 (2016). https://doi.org/10.1155/2016/9278701

[20] Abo-Zahhad, Mohammed, Mohammed Farrag, Abdelhay Ali, and Osama Amin. "An energy consumption model for wireless sensor networks." In *5th International Conference on Energy Aware Computing Systems & Applications*, pp. 1-4. IEEE, 2015. https://doi.org/10.1109/ICEAC.2015.7352200

[21] Kanoun, Olfa. "Energy harvesting for wireless sensor networks." *Technology, Components and System Design*

(2018). https://doi.org/10.1515/9783110445053

[22] Kim, Yong Jun, Hyun Mo Gu, Choong Sun Kim, Hyeongdo Choi, Gyusoup Lee, Seongho Kim, K. Yi Kevin, Sang Gug Lee, and Byung Jin Cho. "High-performance self-powered wireless sensor node driven by a flexible thermoelectric generator." *Energy* 162 (2018): 526-533. https://doi.org/10.1016/j.energy.2018.08.064

[23] Hou, Liqun, Shudong Tan, Zhijuan Zhang, and Neil W. Bergmann. "Thermal energy harvesting WSNs node for temperature monitoring in IIoT." *IEEE Access* 6 (2018): 35243-35249. https://doi.org/10.1109/ACCESS.2018.2851203

[24] Mamat, Mohd Nadzri, and Dahaman Ishak. "Analysis of SEPIC-Boost Converter Using Several PID Feedback Tuning Methods for Renewable Energy Applications." *Journal of Advanced Research in Applied Sciences and Engineering Technology* 26, no. 1 (2022): 105-117. https://doi.org/10.37934/araset.26.1.105117

[25] Khamil, Khairun Nisa, Mohd Faizul Mohd Sabri, Azdiana Md Yusop, Fatimah Al-Zahrah Mohd Sa'at, and Ahmad Nizam Isa. "High cooling performances of H-shape heat sink for thermoelectric energy harvesting system (TEHs) at asphalt pavement." *International Journal of Energy Research* 45, no. 2 (2021): 3242-3256. https://doi.org/10.1002/er.6021

[26] Khamil, Khairun Nisa, Mohd Faizul Mohd Sabri, and Azdiana Md Yusop. "Thermoelectric energy harvesting system (TEHs) at asphalt pavement with a subterranean cooling method." *Energy Sources, Part A: Recovery, Utilization, and Environmental Effects* (2020): 1-17. https://doi.org/10.1080/15567036.2020.1785057

[27] Ruzaimi, A., S. Shafie, W. Z. W. Hassan, N. Azis, M. Effendy Ya'acob, and E. E. Supeni. "Photovoltaic panel temperature and heat distribution analysis for thermoelectric generator application." In *2018 IEEE 5th International Conference on Smart Instrumentation, Measurement and Application (ICSIMA)*, pp. 1-5. IEEE, 2018. https://doi.org/10.1109/ICSIMA.2018.8688801

[28] Sharuddin, Muhammad Syadza, Azdiana Md. Yusop, Ahmad Sadhiqin Mohd Isira, N. F. Kamaruddin, and Khairun Nisa Khamil. "Evaluation of voltage generation and thermal distribution from road using thermoelectric technology." *International Journal of Engineering and Advanced Technology (IJEAT)* 8, no. 6 (2019): 4603-4608.

[29] Khamil, K. N., M. F. M. Sabri, A. M. Yusop, and M. S. Sharuddin. "An evalyuation of TEC and TEG characterization for a road thermal energy harvesting." In *2018 International Conference on Sustainable Energy Engineering and Application (ICSEEA)*, pp. 86-91. IEEE, 2018. https://doi.org/10.1109/ICSEEA.2018.8627113

[30] Johar, Muhammad Akmal, Zulkarnain Yahaya, Omar Mohd Faizan Marwah, Wan Akashah Wan Jamaludin, and Mohamed Najib Ribuan. "Feasibility study of Thermal Electric Generator Configurations as Renewable Energy Sources." In *Journal of Physics: Conference Series*, vol. 914, no. 1, p. 012024. IOP Publishing, 2017. https://doi.org/10.1088/1742-6596/914/1/012024

[31] Baharin, Nuraida'Aadilia, Amir Afiq Arzami, Baljit Singh, Muhammad Fairuz Remeli, Lippong Tan, and Amandeep Oberoi. "Passive flow heat exchanger simulation for power generation from solar pond using thermoelectric generators." In *AIP Conference Proceedings*, vol. 1828, no. 1, p. 020021. AIP Publishing LLC, 2017. https://doi.org/10.1063/1.4979392

[32] Daud, M. M. M., Nursyarizal Bin Mohd Nor, and Taib Ibrahim. "Novel hybrid photovoltaic and thermoelectric panel." In *2012 IEEE International Power Engineering and Optimization Conference Melaka*, Malaysia, pp. 269-274. IEEE, 2012. https://doi.org/10.1109/PEOCO.2012.6230873

[33] Hebei. "TEC1-12706." *Hebei Ltd.* Accessed December 13, 2019. https://peltiermodules.com/peltier.datasheet/TEC1-12706.pdf.

[34] Hidalgo-Leon, Ruben, Javier Urquizo, Christian E. Silva, Jorge Silva-Leon, Jinsong Wu, Pritpal Singh, and Guillermo Soriano. "Powering nodes of wireless sensor networks with energy harvesters for intelligent buildings: A review." *Energy Reports* 8 (2022): 3809-3826. https://doi.org/10.1016/j.egyr.2022.02.280

[35] Charris, Daniela, Diego Gomez, Angie Rincon Ortega, Mauricio Carmona, and Mauricio Pardo. "A thermoelectric energy harvesting scheme with passive cooling for outdoor IoT sensors." *Energies* 13, no. 11 (2020): 2782. https://doi.org/10.3390/en13112782

[36] Kimura, Keisuke, and Hirotaka Koizumi. "A bipolar power converter with bridgeless boost rectifier for thermoelectric energy harvesting." In *2015 IEEE 2nd International Future Energy Electronics Conference (IFEEC)*, pp. 1-6. IEEE, 2015. https://doi.org/10.1109/IFEEC.2015.7361617

[37] Taeda, Keita, and Hirotaka Koizumi. "A bipolar self-Start up boost converter for thermoelectric energy harvesting." In *2017 IEEE Energy Conversion Congress and Exposition (ECCE)*, pp. 4747-4752. IEEE, 2017. https://doi.org/10.1109/ECCE.2017.8096808

[38] Taeda, Keita, Norihiro Shiina, Keisuke Kimura, and Hirotaka Koizumi. "A thermoelectric energy harvesting system with bridgeless boost/buck-boost rectifier." In *IECON 2017-43rd Annual Conference of the IEEE Industrial Electronics Society*, pp. 720-725. IEEE, 2017. https://doi.org/10.1109/IECON.2017.8216125

[39] Kimura, Keisuke, Keita Taeda, Shohei Niikawa, and Hirotaka Koizumi. "A Wireless Sensor Node Driving System with Bridgeless Bipolar Boost Rectifier Using Thermoelectric Energy Harvesting." In *2018 IEEE International Symposium*

on Circuits and Systems (ISCAS), pp. 1-5. IEEE, 2018. https://doi.org/10.1109/ISCAS.2018.8351717